

## Kinetics of electron and proton transfer during O<sub>2</sub> reduction in cytochrome *aa*<sub>3</sub> from *A. ambivalens*: an enzyme lacking Glu(I-286)

Gwen Gilderson<sup>a,c</sup>, Anna Aagaard<sup>a,c</sup>, Cláudio M. Gomes<sup>b</sup>, Pia Ädelroth<sup>1,a</sup>,  
Miguel Teixeira<sup>b</sup>, Peter Brzezinski<sup>a,\*</sup>

<sup>a</sup> Department of Biochemistry, The Arrhenius Laboratories for Natural Sciences, Stockholm University, SE-106 91 Stockholm, Sweden

<sup>b</sup> Instituto de Tecnologia Química e Biológica, Universidade Nova de Lisboa, Rua da Quinta Grande, 6, Apartado 127, 2780-156 Oeiras, Portugal

<sup>c</sup> Department of Biochemistry and Biophysics, Göteborg University (Medicinaregatan 9C), P.O. Box 462, SE-405 30 Göteborg, Sweden

Received 5 April 2000; received in revised form 20 June 2000; accepted 6 July 2000

### Abstract

*Acidianus ambivalens* is a hyperthermoacidophilic archaeon which grows optimally at ~80°C and pH 2.5. The terminal oxidase of its respiratory system is a membrane-bound quinol oxidase (cytochrome *aa*<sub>3</sub>) which belongs to the heme-copper oxidase superfamily. One difference between this quinol oxidase and a majority of the other members of this family is that it lacks the highly-conserved glutamate (Glu(I-286), *E. coli* ubiquinol oxidase numbering) which has been shown to play a central role in controlling the proton transfer during reaction of reduced oxidases with oxygen. In this study we have investigated the dynamics of the reaction of the reduced *A. ambivalens* quinol oxidase with O<sub>2</sub>. With the purified enzyme, two kinetic phases were observed with rate constants of  $1.8 \cdot 10^4 \text{ s}^{-1}$  (at 1 mM O<sub>2</sub>, pH 7.8) and  $3.7 \times 10^3 \text{ s}^{-1}$ , respectively. The first phase is attributed to binding of O<sub>2</sub> to heme *a*<sub>3</sub> and oxidation of both hemes forming the ‘peroxy’ intermediate. The second phase was associated with proton uptake from solution and it is attributed to formation of the ‘oxo-ferryl’ state, the final state in the absence of quinol. In the presence of bound caldariella quinol (QH<sub>2</sub>), heme *a* was re-reduced by QH<sub>2</sub> with a rate of  $670 \text{ s}^{-1}$ , followed by transfer of the fourth electron to the binuclear center with a rate of  $50 \text{ s}^{-1}$ . Thus, the results indicate that the quinol donates electrons to heme *a*, followed by intramolecular transfer to the binuclear center. Moreover, the overall electron and proton-transfer kinetics in the *A. ambivalens* quinol oxidase are the same as those in the *E. coli* ubiquinol oxidase, which indicates that in the *A. ambivalens* enzyme a different pathway is used for proton transfer to the binuclear center and/or other protonatable groups in an equivalent pathway are involved. Potential candidates in that pathway are two glutamates at positions (I-80) and (I-83) in the *A. ambivalens* enzyme (corresponding to Met(I-116) and Val(I-119), respectively, in *E. coli* cytochrome *bo*<sub>3</sub>). © 2001 Elsevier Science B.V. All rights reserved.

**Keywords:** Cytochrome *c* oxidase; Quinol oxidase; Flow flash; Proton pumping; Gating

Abbreviations: R, fully reduced enzyme; A, ferrous-oxy intermediate; P<sub>m</sub> and P<sub>r</sub>, the peroxy intermediate formed upon reaction of the mixed-valence and fully reduced enzyme, respectively, with oxygen; F, oxo-ferryl intermediate; O, fully-oxidized enzyme; Cu<sub>B</sub>, copper B; QH<sub>2</sub>, quinol; WT, wild type; substrate proton, a proton used for reduction of O<sub>2</sub> to water (cf. pumped proton); If not otherwise indicated, the *E. coli* cytochrome *bo*<sub>3</sub> amino-acid residue numbering is used

\* Corresponding author. Fax: +46-8-153679; E-mail: peterb@biokemi.su.se

<sup>1</sup> Present address: Department of Physics, University of California, San Diego, La Jolla, CA 92093-0354, USA.

## 1. Introduction

The hyperthermoacidophilic crenarchaeon *Acidianus ambivalens* is a member of the Sulfolobales, that grows optimally at  $\sim 80^\circ\text{C}$  and pH 2.5 [1,2]. When using colloidal sulfur as an electron donor and oxygen as an acceptor it expresses a very simple membrane-bound respiratory system. The terminal oxidase of this system is a quinol oxidase which is the major membrane-bound heme-chromophore [3,4]. The oxidase has a molecular mass of 150 kDa and it is composed of five subunits, the largest of which (65 kDa) contains the ligands to heme *a* and the binuclear center heme *a*<sub>3</sub> and Cu<sub>B</sub> [5]. The enzyme receives electrons from caldariella quinol [3,4], which are transferred intramolecularly to the binuclear center where oxygen binds and is reduced to water. The bound quinol has been shown to be essential to complete the oxygen reaction [4] and to modulate a conformational change at the binuclear site upon reduction, which may be correlated to the proton pumping mechanism of this oxidase [6]. The structures at atomic resolution of two other oxidases belonging to the same heme-copper oxidase superfamily as the *A. ambivalens* enzyme have been determined: cytochrome *c* oxidase from bovine heart [7–9] and *Paracoccus denitrificans* [10,11].

The reaction with O<sub>2</sub> of several cytochrome *c* oxidases and the ubiquinol oxidase cytochrome *bo*<sub>3</sub> from *Escherichia coli* have been investigated in detail using the so-called flow-flash technique (for a review see, e.g., [12,13]). The reduced enzyme with carbon monoxide bound to heme *a*<sub>3</sub> (heme *o*<sub>3</sub>) is mixed rapidly with an O<sub>2</sub>-containing solution. The reaction of the reduced enzyme with O<sub>2</sub> is limited by the CO-off rate. Within a time frame that is shorter than that of CO dissociation, the CO ligand is flashed off with a short laser flash which enables O<sub>2</sub> to react with the reduced enzyme. With both the bovine cytochrome *aa*<sub>3</sub> and *E. coli* cytochrome *bo*<sub>3</sub>, initially, O<sub>2</sub> binds to reduced heme *a*<sub>3</sub> (heme *o*<sub>3</sub>) with a rate of  $\sim 10^5 \text{ s}^{-1}$  (at 1 mM O<sub>2</sub>, forming transient intermediate A) [14,15]. In the next step both hemes *a* and *a*<sub>3</sub> (heme *b* and heme *o*<sub>3</sub>) are oxidized forming the so-called ‘peroxy’ intermediate (P) with a rate of  $\sim 3 \times 10^4 \text{ s}^{-1}$  [16–19]. The ‘oxo-ferryl’ (F) intermediate is formed with a rate of  $\sim 10^4 \text{ s}^{-1}$ , associated with proton uptake from solution through the D-pathway

[20–22] including the highly-conserved Glu(I-286) and Asp(I-132). In cytochrome *c* oxidase, the fourth electron is transferred to the binuclear center, a proton is taken up through the D-pathway and the oxidized enzyme (O) is formed with a rate of  $\sim 10^3 \text{ s}^{-1}$ . Quinol oxidases lack the Cu<sub>A</sub> center and have only three redox-active metal sites [23]. Thus, during reaction of the fully-reduced *E. coli* ubiquinol oxidase with O<sub>2</sub> the final state is F [20,24]. The same situation was observed for the *A. ambivalens* enzyme [4]. With bound quinol in the *E. coli* cytochrome *bo*<sub>3</sub>, heme *b* is re-reduced rapidly by QH<sub>2</sub> after the initial oxidation of heme *b*, which is followed by transfer of the fourth electron from heme *b* to the binuclear center [17,18].

Numerous studies show that the D-pathway is involved in the uptake of both substrate and pumped protons during reduction of oxygen to water in mitochondrial-like oxidases (for review see [25]). The *A. ambivalens* quinol oxidase lacks many of the key residues in this pathway, including the essential glutamate E(I-286) and it has been suggested that the *A. ambivalens* enzyme generates a proton gradient only by ‘chemical’ charge separation [5], i.e., only through the uptake of substrate protons specifically from the ‘input side’ of the membrane. Thus, one question addressed in this work is the kinetics of proton uptake during O<sub>2</sub> reduction. To approach this problem we have employed the flow-flash technique to investigate the kinetics of electron and proton transfer during reaction of the fully-reduced *A. ambivalens* cytochrome *aa*<sub>3</sub> with oxygen. The results show that the reduced enzyme reacts with O<sub>2</sub> on a microsecond time scale. Initially, both hemes *a* and *a*<sub>3</sub> were oxidized with a rate of  $1.8 \times 10^4 \text{ s}^{-1}$ , presumably forming intermediate P. A proton was taken up from the bulk solution and the F intermediate was formed with a rate of  $3.7 \times 10^3 \text{ s}^{-1}$ . In the presence of caldariella quinol (in the solubilized membrane extract), heme *a* was re-reduced by the quinol with a rate of  $670 \text{ s}^{-1}$ , followed by transfer of the fourth electron from heme *a* to the binuclear center with a rate of  $50 \text{ s}^{-1}$ . Thus, the results show that the caldariella quinol first donates electrons to heme *a*, which are then transferred intramolecularly to the binuclear center. Moreover, the *A. ambivalens* quinol oxidase picks up protons from solution with the same rate as the *E. coli* ubiquinol oxidase (and cyto-

chrome *c* oxidases from bovine heart and *R. sphaeroides*), which indicates that other residues (presumably carboxylates) in the *A. ambivalens* oxidase play the role of Glu(I-286).

## 2. Materials and methods

### 2.1. Enzyme purification

*A. ambivalens* (DSM 3772) cells were grown as described in [26] and the membranes and the purified oxidase were obtained as previously described [4]. The solubilized membrane extract was prepared by adding dodecyl- $\beta$ -D-maltoside to a membrane suspension at a ratio of 2 g of detergent per g of total protein, in potassium phosphate buffer at pH 6.5. After mixing at 4°C for 3 h the suspension was ultracentrifuged to remove unsolubilized membranes. The purified enzyme is almost fully depleted of quinone, as determined from quinone extraction and HPLC analysis (our unpublished data). The enzyme concentration was determined from the reduced-minus-oxidized difference spectrum using an absorption coefficient of 23.2 mM<sup>-1</sup>cm<sup>-1</sup> at 605 nm [27].

### 2.2. Flow-flash measurements

The solution of the reduced quinol oxidase–CO complex (see [28]) was transferred anaerobically to one of the drive syringes (volume 500  $\mu$ l) of a locally modified stopped-flow apparatus (Applied Photophysics, DX-17MV). The other syringe (volume 2.5 ml) was filled with the same buffer solution supplemented with 0.1% dodecyl- $\beta$ -D-maltoside, equilibrated with pure O<sub>2</sub> at 1 atm. Typically, the enzyme/O<sub>2</sub>-solution mixing ratio of 1:5 gave an O<sub>2</sub> concentration after mixing of  $\sim$ 1 mM. Actinic light at 532 nm was provided by a Nd-YAG laser (Spectra Physics) about 40 ms after mixing. The pulse length was  $\sim$ 10 ns and the energy per pulse was  $\sim$ 50 mJ. Typically, 5–20 traces were averaged. The laser and observation equipment have been described in detail elsewhere [16]. The concentration of reacting enzyme was calculated from the CO-dissociation absorbance change at 445 nm, using an absorption coefficient of 67 mM<sup>-1</sup>cm<sup>-1</sup> [29].

### 2.3. Proton-uptake measurements

The kinetics of proton uptake during O<sub>2</sub> reduction was measured as described previously [16,21]. The buffer was removed from the enzyme solution by washing two times with 0.1 M KCl, 0.1%  $\beta$ -D-dodecyl maltoside at pH 7.5 on a PD-10 column (Pharmacia). The pH dye phenol red at a final concentration of 40  $\mu$ M was added after which the enzyme solution was flushed with nitrogen. To reduce the enzyme, ascorbate and phenazine methosulfate (PMS) were added to final concentrations of 1 mM and 5  $\mu$ M, respectively. After incubation for  $\sim$ 10 h at +4°C, nitrogen was exchanged for carbon monoxide and the pH was adjusted to 7.8. The measurements were performed as described above and in [16]. A relation between the observed absorbance changes and the number of protons taken up by the enzyme (cf. buffer capacity) was determined as described elsewhere [16].

## 3. Results

### 3.1. Reaction of the purified enzyme with O<sub>2</sub> electron transfer

The enzyme–CO complex was mixed in a stopped-flow apparatus with an O<sub>2</sub>-saturated solution. The CO ligand was flashed off about 40 ms after mixing. Since the CO-off rate from heme *a*<sub>3</sub> was  $\sim$ 1 s<sup>-1</sup> under the current experimental conditions, during the time between mixing and the flash  $\sim$ 4% of the enzyme with CO bound to heme *a*<sub>3</sub> reacted (see also below). In contrast to the bovine cytochrome *aa*<sub>3</sub> in which CO binds to heme *a*<sub>3</sub> in the entire enzyme population, in the *A. ambivalens* quinol oxidase the ligand equilibrates between heme *a*<sub>3</sub> and Cu<sub>B</sub>, with about 40% of the enzyme population having CO bound to Cu<sub>B</sub> [28]. Since the CO-dissociation time constant from Cu<sub>B</sub> is much shorter ( $\sim$ 100  $\mu$ s, [28]) than the time between mixing and the laser flash (40 ms), the enzyme population in which CO is bound to Cu<sub>B</sub> reacts with O<sub>2</sub> before the flash and does not contribute to the light-induced absorbance changes (see also Section 4).

Fig. 1 shows absorbance changes following flash-induced dissociation of CO from the *A. ambivalens*

quinol oxidase (from the population in which CO is bound to heme  $a_3$ ) after mixing with an  $O_2$ -saturated solution in a stopped-flow apparatus. At 445 nm (Fig. 1A), the increase in absorbance at  $t=0$  is associated with dissociation of CO from heme  $a_3$ . It is followed by a decrease in absorbance with a rate constant<sup>2</sup> of  $1.8 \pm 0.4 \times 10^4 \text{ s}^{-1}$  at pH 7.8, associated with oxidation of hemes  $a$  and  $a_3$  and presumably formation of the so-called peroxy intermediate (**P**). The yield of CO dissociation was  $< 100\%$ . Since the enzyme fraction in which CO does not dissociate reacts with  $O_2$  with a rate of  $\sim 1 \text{ s}^{-1}$  (see above), the absorbance changes of this fraction do not contribute on the time scale in Fig. 1.

Since the purified *A. ambivalens* enzyme ‘contains’ three electrons, upon reaction with  $O_2$ , the final state is expected to be the oxo-ferryl intermediate (**F**) [4]. This intermediate has its maximum contribution (compared with the oxidized enzyme) at 580 nm. At this wavelength the absorbance increased with a rate constant of  $3.7 \pm 0.4 \times 10^3 \text{ s}^{-1}$  at pH 7.8 (determined from a global fit of the data, see <sup>2</sup>) (Fig. 1B), which in the bovine and *R. sphaeroides* cytochrome  $aa_3$  is characteristic for the formation of the **F** intermediate [16,21]. In addition, a small component with a rate constant of  $\sim 650 \text{ s}^{-1}$  was observed, presumably due to a small fraction tightly bound caldariella quinol, which cannot be displaced by stigmatellin (see below). The rate of the first phase following that associated with CO dissociation, tentatively ascribed to formation of the **P** intermediate was the same at pH 5 as at pH 7.8.

Fig. 2A shows the apparent first-order rate constant of the kinetic phase immediately after CO dissociation as a function of the  $O_2$  concentration. As seen in the figure, the rate constant first increases with increasing  $O_2$  concentration and then it saturates. The curve was fitted with a hyperbolic function (solid line in Fig. 2A):

$$k_{\text{obs}} = \frac{k_{\text{max}}[O_2]}{K_{\text{m,app}} + [O_2]} \quad (1)$$

<sup>2</sup> The rate constants of the kinetic phases were determined from a multi-wavelength fit to traces collected at eight different wavelengths: 420, 430, 436, 437, 445, 580, 600 and 605 nm. In addition, absorbance changes at 560 nm associated with proton uptake were included in the global fit.

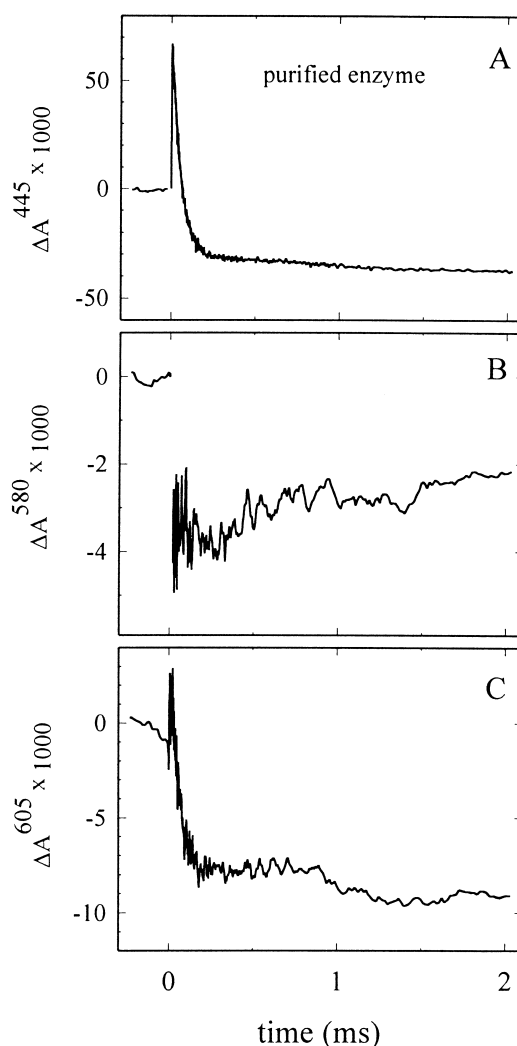


Fig. 1. Absorbance changes after flash photolysis of CO from the fully-reduced purified *A. ambivalens* quinol oxidase after rapid mixing with an  $O_2$ -saturated solution at a ratio of 1:5 (A) 445 nm; (B) 580 nm; (C) 605 nm. Conditions after mixing: 100 mM potassium phosphate buffer, pH 7.8, 0.1% dodecyl- $\beta$ -D-maltoside, 2 mM sodium ascorbate, 5  $\mu\text{M}$  phenazine methosulfate (PMS),  $\sim 170 \mu\text{M}$  CO,  $\sim 1 \text{ mM}$   $O_2$ ,  $22 \pm 1^\circ\text{C}$ . The enzyme concentration was 10–15  $\mu\text{M}$ , but all traces have been normalized to 1  $\mu\text{M}$  reacting enzyme (normalized to the CO dissociation absorbance change at 445 nm using  $\epsilon = 67 \text{ mM}^{-1} \text{ cm}^{-1}$  [29]).

with values  $k_{\text{max}} = 1.8 \pm 0.2 \times 10^4 \text{ s}^{-1}$  and  $K_{\text{M,app}} = 65 \pm 15 \mu\text{M}$  (see also model in Fig. 2B, discussed below). The initial slope at low  $O_2$  concentrations corresponds to a second-order rate constant of  $2.7 \pm 1.0 \times 10^8 \text{ M}^{-1} \text{ s}^{-1}$ , i.e., similar to those observed with the bovine and *R. sphaeroides* cytochrome  $c$  oxidases, and the *E. coli* cytochrome  $bo_3$

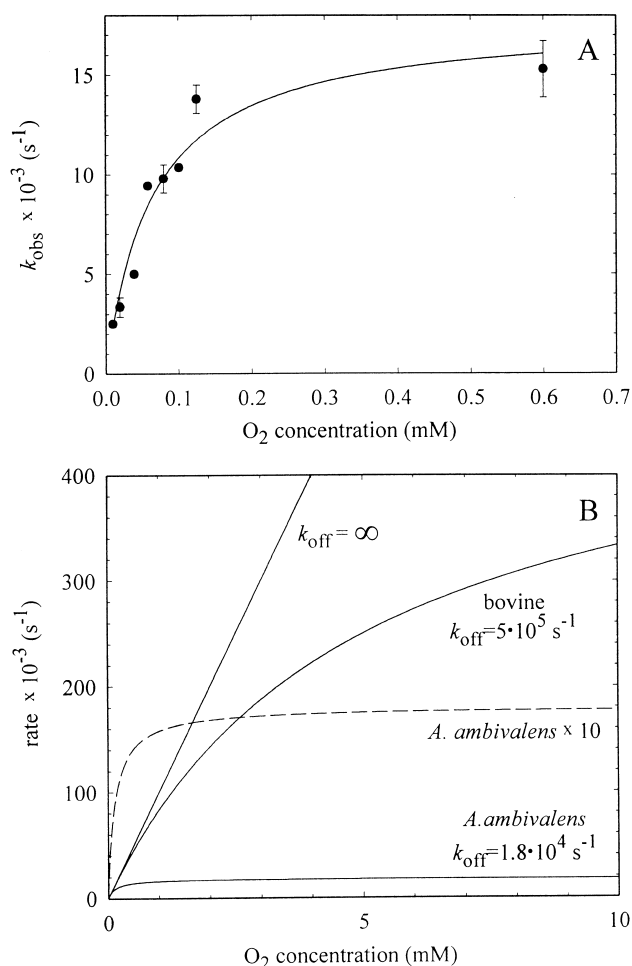


Fig. 2. (A) The rate of the initial kinetic phase after CO-dissociation, measured at 445 nm (flow-flash experiment) as a function of the  $O_2$  concentration after mixing in the flow-flash apparatus. Conditions were the same as in Fig. 1, except that mixing ratio was 1:1 and the  $O_2$  concentration was varied as indicated in the figure. (B) Simulated curves for  $O_2$  binding to heme  $a_3$  with a second-order rate constant of  $10^8 \text{ M}^{-1} \text{ s}^{-1}$ , limited by the CO-off rate from  $Cu_B$  (different values of  $k_{\text{off}}$  c.f.  $k_{\text{max}}$  in Eq. 1). As seen in the Figure, a small  $k_{\text{off}}$  gives a small apparent  $K_m$  value (see Eq. 1).

( $\sim 1.4 \times 10^8 \text{ M}^{-1} \text{ s}^{-1}$ , with the bovine enzyme) [16,30,31].

### 3.2. Reaction of the purified enzyme with $O_2$ proton uptake

The kinetics of proton uptake associated with  $O_2$  reduction by the purified enzyme was investigated by monitoring absorbance changes at 560 nm of the pH-indicator dye phenol red in the absence of buffer. To

correct for the small contribution of the enzyme absorbance at 560 nm, absorbance changes were also recorded in the presence of buffer. The difference trace (Fig. 3) displayed the same rate constant of  $3.7 \times 10^3 \text{ s}^{-1}$  as that attributed to the  $P \rightarrow F$  transition (see above). As in the experiments described above, a small component ( $\sim 10\%$  of the total absorbance change) with a rate of  $650 \text{ s}^{-1}$  was observed.

### 3.3. Reaction of the membrane quinol-bound enzyme with $O_2$

As discussed in Section 1, the major heme chromophore in the membrane fragments from *A. ambivalens* is the quinol oxidase, cytochrome  $aa_3$ . Thus, it is possible to investigate the reaction of the fully-reduced enzyme with  $O_2$  using optical absorption spectroscopy also with the enzyme in the membrane extract without interference from absorbance changes originating from other protein complexes. Previous studies have shown that in this state the enzyme fully reduces oxygen to water, using bound quinol [4,6].

Fig. 4 shows absorbance changes following flash-

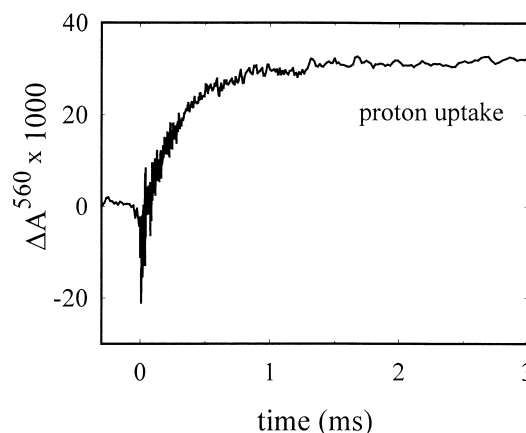


Fig. 3. Proton uptake associated with reaction of the reduced, purified *A. ambivalens* quinol oxidase with  $O_2$ . The figure shows absorbance changes of the dye phenol red at 560 nm. An increase in absorbance reflects proton uptake. The trace is the differences of the traces obtained in non-buffered and buffered solutions at pH 7.8. Experimental conditions were the same as in Fig. 1, except that in the buffer-free solution, the sample was supplemented with 0.1 M KCl, the concentration of phenol red was  $40 \mu\text{M}$  and the enzyme concentration was  $25\text{--}30 \mu\text{M}$ . The absorbance change corresponds to an uptake of  $\sim 1\text{H}^+$ /enzyme molecule.

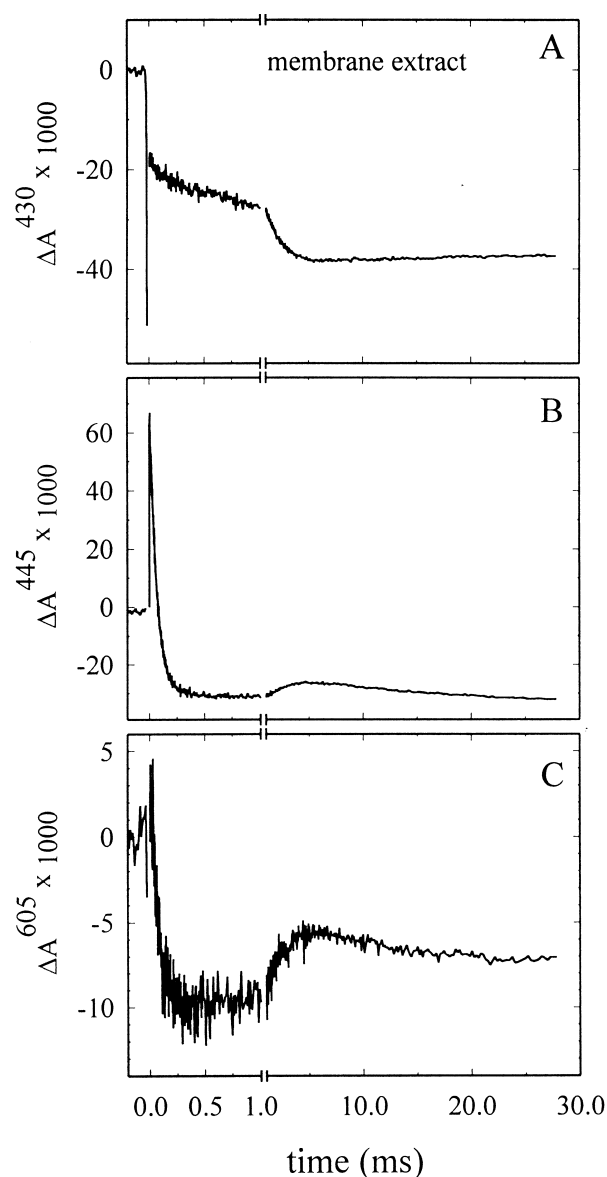


Fig. 4. Absorbance changes after flash photolysis of CO from the fully-reduced *A. ambivalens* quinol oxidase in the membrane extract after rapid mixing with an  $O_2$ -saturated solution at (A) 430 nm; (B) 445 nm; (C) 605 nm. See Fig. 1 for details. Conditions were the same as in Fig. 1, except that the potassium phosphate concentration was 50 mM (pH 7.8) and the dodecyl- $\beta$ -D-maltoside concentration was 5%.

induced CO dissociation from the membrane extract quinol oxidase in the presence of  $O_2$ . At 445 nm (Fig. 4B), the initial absorbance changes were the same as those observed with the purified enzyme, i.e., a rapid increase in absorbance, associated with CO dissociation; these changes were followed by a decrease in absorbance with a rate constant of  $\sim 1.5 \times 10^4 \text{ s}^{-1}$ ,

associated with oxidation of both hemes and presumably formation of the **P** intermediate. However, in contrast to the absorbance changes observed with the purified enzyme, in the membrane-extract we observed an increase in absorbance at 445 nm and 605 nm and a decrease in absorbance at 430 nm with a rate constant of  $670 \text{ s}^{-1}$ , attributed to re-reduction of heme *a* by the bound quinol (Fig. 4 c.f. Fig. 1). This kinetic phase was followed by a slower change in absorbance with a rate constant of  $50 \text{ s}^{-1}$ , attributed to the transfer of the fourth electron to the binuclear center forming state **O**.

Qualitatively, the same behavior was observed previously with the ubiquinol-containing cytochrome *bo3* from *E. coli* [17,18], in which the electron was transferred from the protein-bound quinol to heme *b* with a rate of  $1.4 \times 10^3 \text{ s}^{-1}$ , followed by transfer of the fourth electron to the binuclear center forming the oxidized enzyme (state **O**) with a rate of  $250 \text{ s}^{-1}$  [18].

#### 4. Discussion

In this study we have investigated the reaction of the fully-reduced quinol oxidase from *Acidianus ambivalens* with oxygen, in the purified form as well as in membrane extracts. We have previously shown that in the fully-reduced enzyme, the heme *a*<sub>3</sub>-CO complex is formed in about 60% of the enzyme population. Assuming that only one CO molecule can bind to each enzyme molecule, in the remaining population, CO is bound to  $Cu_B$ . Upon mixing of the enzyme-CO complex with oxygen the enzyme fraction in which CO is bound to  $Cu_B$  reacts with  $O_2$  on a time scale of  $\sim 100 \mu\text{s}$  because the CO-off rate from  $Cu_B$  is  $\sim 1.4 \times 10^4 \text{ s}^{-1}$  [28]. In the remaining enzyme population, in the dark, the reaction rate is limited by the CO-off rate from heme *a*<sub>3</sub> of  $\sim 1 \text{ s}^{-1}$ , which allows the use of the flow-flash methodology for the investigation of the reaction of the reduced enzyme with  $O_2$ , provided that CO is flashed off within a time much shorter than 1 s after mixing.

The reactions of the fully-reduced bovine and *R. sphaeroides* cytochrome *c* oxidases with  $O_2$  have been investigated in detail previously (see, e.g., [12,13,16]). On the basis of a comparison of the absorbance changes observed with these enzymes and the *A. am-*

*bivalens* cytochrome *aa*<sub>3</sub>, the initial decrease in absorbance at 445 nm (Fig. 1A) after the CO-dissociation absorbance change, is attributed to binding of O<sub>2</sub>, oxidation of both hemes and formation of intermediate **P** with a rate constant of  $1.8 \times 10^4 \text{ s}^{-1}$ . With the bovine and *R. sphaeroides* enzymes, formation of intermediate **F** can be detected in the alpha region of the spectrum as a slight increase in absorbance at 580 nm where the **F** intermediate has its maximum absorbance relative to that of the oxidized enzyme. If the reaction stops at intermediate **P** (e.g., in the EQ(I-286) mutant of the *R. sphaeroides* enzyme), instead a significant decrease in absorbance is observed [21]. With the *A. ambivalens* enzyme, a small increase in absorbance was observed at 580 nm (and there was no decrease in absorbance) (Fig. 1B), which is attributed to formation of the **F** intermediate. This is also confirmed by the observation of proton uptake from solution with a rate constant of  $\sim 3.7 \times 10^3 \text{ s}^{-1}$  (Fig. 3). Formation of the **F** intermediate was also detected after rapid mixing of the fully reduced enzyme with dioxygen [4].

When the same experiment was done with the enzyme in the membrane extract, containing bound caldariella quinol, additional kinetic phases with rates of  $670 \text{ s}^{-1}$  and  $50 \text{ s}^{-1}$  were observed, presumably associated with electron transfer from QH<sub>2</sub> to heme *a* (increase in absorbance at 445 nm and 605 nm, and decrease in absorbance at 430 nm, see Fig. 4) and the transfer of the fourth electron from heme *a* to the binuclear center (decrease in absorbance at 445 nm and 605 nm, see Fig. 4), respectively.

In cytochrome *c* oxidase the re-reduction of heme *a* by Cu<sub>A</sub> displays the same rate constant ( $\sim 10^4 \text{ s}^{-1}$ ) as the **P**→**F** transition and proton uptake from solution. In the *A. ambivalens* cytochrome *aa*<sub>3</sub> the electron transfer from quinol to heme *a* is slower than the **P**→**F** transition, presumably because the electron-transfer rate is limited by proton release from QH<sub>2</sub> with a rate of  $670 \text{ s}^{-1}$  (see [18]). It is difficult to quantify the observed absorbance changes associated with this phase because we were not able to determine the fraction of enzyme with bound quinol accurately.

After the  $50\text{-s}^{-1}$  electron transfer from heme *a* to the binuclear center, heme *a* is re-reduced by the 'second electron' from the quinol (fifth electron in the enzyme), which equilibrates between the semiqui-

none state and the redox centers of the enzyme. This explains why the  $50 \text{ s}^{-1}$  decrease in absorbance at 445 nm and 605 nm is relatively small (Fig. 4). Qualitatively, a similar behavior was observed previously with the ubiquinol-containing quinol oxidase cytochrome *bo*<sub>3</sub> from *E. coli* [17,18] in which electrons from ubiquinol are donated to the low-spin heme *b* and then to the oxygen-reducing binuclear center heme *o*<sub>3</sub>-Cu<sub>B</sub> [17,18].

In the bovine enzyme O<sub>2</sub> binds to heme *a*<sub>3</sub> with a second-order rate constant of  $1.4 \times 10^8 \text{ M}^{-1} \text{ s}^{-1}$  forming the ferrous-oxo intermediate (**R**→**A** transition). Thus, at 1 mM O<sub>2</sub> (and  $\mu\text{M}$  enzyme concentrations), the apparent first-order rate constant is  $\sim 10^5 \text{ s}^{-1}$  [15,30,31]. With the bovine enzyme, the kinetic phase associated with O<sub>2</sub> binding (formation of intermediate **A**) is observed as a decrease in absorbance at 445 nm immediately following dissociation of CO. The O<sub>2</sub> binding is followed by the further decrease in absorbance with a rate of  $3 \times 10^4 \text{ s}^{-1}$  associated with oxidation of the hemes and formation of the **P** intermediate. At lower O<sub>2</sub> concentrations the two phases merge and below  $\sim 300 \mu\text{M}$  O<sub>2</sub> the **P**-formation rate is limited by O<sub>2</sub> binding to heme *a*<sub>3</sub>. Consequently, the slope of the apparent **P** formation rate as a function of O<sub>2</sub> concentration at low O<sub>2</sub> concentrations reflects the second-order rate constant for binding of O<sub>2</sub>. As seen in Fig. 2A, the slope with the *A. ambivalens* enzyme corresponds to a second-order rate constant for O<sub>2</sub> binding of  $\sim 2.7 \times 10^8 \text{ M}^{-1} \text{ s}^{-1}$  (see Eq. 1), i.e., similar to that observed with the bovine cytochrome *aa*<sub>3</sub>.

If there were no other rate-limiting events for O<sub>2</sub> binding in the *A. ambivalens* enzyme and if the **A** intermediate was formed at significant concentrations (see below), at 1 mM O<sub>2</sub> a kinetic phase associated with **A** formation with a rate constant of  $\sim 2.7 \times 10^5 \text{ s}^{-1}$  should be observed. With the bovine enzyme, the two initial phases ( $10^5 \text{ s}^{-1}$  and  $3 \times 10^4 \text{ s}^{-1}$ , **R**→**A** and **A**→**P**, respectively, at 1 mM O<sub>2</sub>) have the same sign at 445 nm. Since their rates differ only by a factor of  $\sim 3$  at 1 mM O<sub>2</sub>, it is often difficult to resolve them at this wavelength. However, in the range  $\sim 430\text{--}440 \text{ nm}$  there are wavelengths at which the two phases display different signs. In addition, there are wavelengths at which each of them displays an isosbestic point, which simplifies their resolution [30]. With the *A. ambivalens* quinol oxidase we were not able to

resolve the O<sub>2</sub>-binding phase in this wavelength range.

There are several possible explanations for the lack of a resolved O<sub>2</sub>-binding phase in the *A. ambivalens* quinol oxidase. One possibility is the relatively slow CO-dissociation rate from Cu<sub>B</sub> in the *A. ambivalens* enzyme ( $1.4 \pm 0.5 \times 10^4 \text{ s}^{-1}$  [28]). With the bovine enzyme it has been proposed that the CO-dissociation from Cu<sub>B</sub> is rate-limiting for O<sub>2</sub> binding. In a study of the O<sub>2</sub> binding rate as a function of O<sub>2</sub> concentration at O<sub>2</sub> concentrations up to 16 mM [31], a saturation behavior was found, similar to that observed with the *A. ambivalens* enzyme (Fig. 2A). With the bovine enzyme, the rate saturated at  $\sim 10^6 \text{ s}^{-1}$  [31], which is consistent with the CO-dissociation rate of  $\sim 5 \times 10^5 \text{ s}^{-1}$  [32]. Consequently, it was proposed that the saturation behavior at high O<sub>2</sub> concentrations reflects the (rate-limiting) CO dissociation from Cu<sub>B</sub>. Since with the bovine enzyme the CO-dissociation rate ( $5 \times 10^5 \text{ s}^{-1}$ ) is faster than that of O<sub>2</sub> binding at 1 mM O<sub>2</sub> ( $\sim 1 \times 10^5 \text{ s}^{-1}$ ) and much faster than the **A** → **P** transition there is essentially no interference between CO dissociation and O<sub>2</sub> binding at this O<sub>2</sub> concentration and a kinetic phase associated with O<sub>2</sub> binding to heme *a*<sub>3</sub> is clearly resolved [30].

Also with the *A. ambivalens* cytochrome *aa*<sub>3</sub> the apparent O<sub>2</sub>-binding rate saturated at about the same value ( $k_{\text{max}} \cong 1.8 \times 10^4 \text{ s}^{-1}$ , see Eq. 1) as the CO dissociation rate from Cu<sub>B</sub> ( $\sim 1.4 \times 10^4 \text{ s}^{-1}$ ). However, since this rate is much slower than the expected rate for O<sub>2</sub> binding at 1 mM O<sub>2</sub> and presumably also the **A** → **P** transition, in the *A. ambivalens* cytochrome *aa*<sub>3</sub> the **P** formation rate is determined by the CO dissociation. In addition, due to the slower CO dissociation rate in the *A. ambivalens* than in the bovine enzyme, the apparent *K<sub>m</sub>* value for O<sub>2</sub> binding is much smaller in the *A. ambivalens* ( $\sim 65 \mu\text{M}$ ) than in the bovine (7.7 mM, [31]) enzyme (see Fig. 2B).

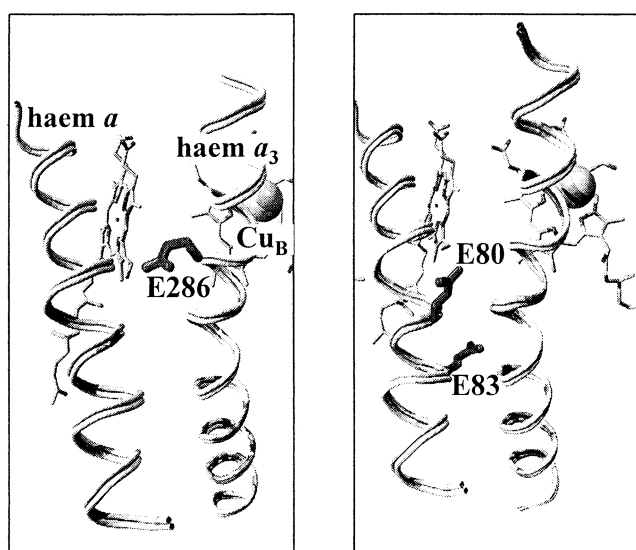
Also in the ubiquinol oxidase from *E. coli*, after dissociation of CO from the reduced enzyme (heme *o*<sub>3</sub>), CO binds transiently to Cu<sub>B</sub> and dissociates with a time constant of  $\sim 1 \text{ ms}$  [33,34]. On the other hand, O<sub>2</sub> reacts with the fully-reduced *E. coli* enzyme with a rate of  $\sim 10^5 \text{ s}^{-1}$  (at 1 mM O<sub>2</sub>) [14,20,35], which seemingly contradicts the requirement for CO to dissociate before O<sub>2</sub> binding (see also discussion in

[34]). Thus, it is possible that O<sub>2</sub> can bind to heme *o*<sub>3</sub> (heme *a*<sub>3</sub>) even though CO is bound to Cu<sub>B</sub>. However, even if this is the case the O–O bond cannot be cleaved until CO dissociates from Cu<sub>B</sub> because the O–O bond breakage requires binding of OH<sup>−</sup> (H<sub>2</sub>O) to Cu<sub>B</sub>. Therefore, in the *A. ambivalens* enzyme formation of **P** (in which the O–O bond is cleaved, see e.g., [36]) is rate-limited by CO dissociation. Also, a direct binding of O<sub>2</sub> to heme *a*<sub>3</sub> is likely to be slowed by the presence of CO at Cu<sub>B</sub>.

The  $10^4 \text{ s}^{-1}$  proton uptake during the **P** → **F** transition in the *R. sphaeroides* cytochrome *c* oxidase takes place through the D-pathway (for review see [25]) in which one of the key residues is Glu(I-286). Replacement of the Glu by a Gln in the *R. sphaeroides* enzyme results in blockage of the  $10^4 \text{ s}^{-1}$  proton uptake and inhibition of the **P** → **F** transition. The latter is most likely blocked because formation of the **F** intermediate requires an internal proton transfer to the binuclear center [22]. In the *R. sphaeroides* cytochrome *c* oxidase this proton is presumably taken from E(I-286) with a rate of  $10^4 \text{ s}^{-1}$ , followed by a rapid ( $> 10^4 \text{ s}^{-1}$ ) re-protonation of E(I-286) from the bulk solution [22,37]. The proton uptake during the **P** → **F** transition was also observed with the *A. ambivalens* enzyme with a rate of  $3.7 \times 10^3 \text{ s}^{-1}$ , i.e., similar to that observed with the *R. sphaeroides*, bovine and *E. coli* oxidases.

The *A. ambivalens* quinol oxidase lacks the amino-acid residue corresponding to E(I-286) (as well as all the other amino-acid residues of the D-pathway), which indicates that other residues must play a central role in proton transfer in the *A. ambivalens* enzyme (see below). Also in other enzymes related to the mitochondrial-type enzymes, alternative proton transfer pathways are operative (see e.g. [38]). For example, the *caa*<sub>3</sub> oxidase from *Thermus (Th.) thermophilus* has all the residues of the D-pathway conserved, with the exception of the glutamate [39], but pumps protons with the stoichiometry of 1H<sup>+</sup> per electron [40]. This enzyme is part of a subgroup of the mitochondrial-type terminal oxidases which have a conserved substitution pattern in helix VI, YSHPXV, instead of XGHPEV. Homology modeling of one of these enzymes, the *caa*<sub>3</sub> oxidase from *Rhodothermus marinus*, showed that the tyrosine residue may occupy a spatial position equivalent to that of the glutamate residue, thus being proposed to be





## bovine

*A. ambivalens*

Fig. 5. Structural model of the *A. ambivalens* quinol oxidase (right) constructed using the *P. denitrificans* cytochrome *c* oxidase as a model, shown together with the structure of the bovine enzyme (left) [9]. Parts of the D-pathway are shown. In the mitochondrial-like oxidases, E(I-286) (*E. coli* numbering) plays a central role in proton transfer through the D-pathway. This residue is not found in the *A. ambivalens* enzyme. However, as shown in the model, there are two other glutamates (E(I-80) and E(I-83), *A. ambivalens* numbering), E(I-80) having the carboxylate group at about the same position in space as that of E(I-286).

its functional substitute [41]. Also, the cytochromes *ba(o)<sub>3</sub>* from *Th. thermophilus* and *Bacillus stearothermophilus*, which lack the canonical D-pathway, are indeed proton pumps [42,43]. Therefore, it is clear that oxidases have different molecular strategies to achieve proton transfer.

Modeling of the three-dimensional structure of the *A. ambivalens* quinol oxidase (Fig. 5) shows that even though the residue corresponding to E(I-286) at helix VI is not present, there is another glutamate at about the same position in space, but bound to a different helix (Glu (I-80) *A. ambivalens* numbering, Met(I-116) in *E. coli* cytochrome *bo<sub>3</sub>*, Fig. 5). In the structural model, there is also another glutamate (E(I-83)), *A. ambivalens* numbering, Val(I-119) in *E. coli* cytochrome *bo<sub>3</sub>* 'below' the I-286 position (*E. coli* cytochrome *bo<sub>3</sub>* numbering, see Fig. 5). Thus, it is possible that the residues E(I-80) and/or E(I-83) in the *A. ambivalens* enzyme may be part of the proton

transfer pathway to the binuclear center in this oxidase.

## Acknowledgements

We would like to thank A. Kannt and H. Michel, Max-Planck-Institut für Biophysik, Frankfurt, for preparation of a molecular model of the *A. ambivalens* cytochrome *aa<sub>3</sub>*. Supported by grants to P.B. from the Swedish Natural Science Research Council, The Swedish Foundation for International Co-operation in Research and Higher Education (STINT), to M.T. from Praxis XXI (36/97) and to C.M.G. from EMBO.

## References

- [1] W. Zillig, S. Yeats, I. Holz, A. Böck, M. Rettenberger, F. Gropp, G. Simon, Syst. Appl. Microbiol. 8 (1986) 197–203.
- [2] T. Fuchs, H. Huber, S. Burggraf, K.O. Stetter, Syst. Appl. Microbiol. 19 (1996) 56–60.
- [3] S. Anemüller, C.L. Schmidt, I. Pacheco, G. Schäfer, M. Teixeira, FEMS Microbiol. Lett. 117 (1994) 275–280.
- [4] A. Giuffrè, C.M. Gomes, G. Antonini, E. D'Itri, M. Teixeira, M. Brunori, Eur. J. Biochem. 250 (1997) 383–388.
- [5] W.G. Porschke, C.L. Schmidt, A. Petersen, G. Schäfer, J. Bacteriol. 179 (1997) 1344–1353.
- [6] T.K. Das, C.M. Gomes, M. Teixeira, D.L. Rousseau, Proc. Natl. Acad. Sci. USA 96 (1999) 9591–9596.
- [7] T. Tsukihara, H. Aoyama, E. Yamashita, T. Tomizaki, H. Yamaguchi, K. Shinzawa-Itoh, R. Nakashima, R. Yaono, S. Yoshikawa, Science 272 (1996) 1136–1144.
- [8] T. Tsukihara, H. Aoyama, E. Yamashita, T. Tomizaki, H. Yamaguchi, K. Shinzawa-Itoh, R. Nakashima, R. Yaono, S. Yoshikawa, Science 269 (1995) 1069–1074.
- [9] S. Yoshikawa, K. Shinzawa-Itoh, R. Nakashima, R. Yaono, E. Yamashita, N. Inoue, M. Yao, M.J. Fei, C.P. Libeu, T. Mizushima, H. Yamaguchi, T. Tomizaki, T. Tsukihara, Science 280 (1998) 1723–1729.
- [10] S. Iwata, C. Ostermeier, B. Ludwig, H. Michel, Nature 376 (1995) 660–669.
- [11] C. Ostermeier, A. Harrenga, U. Ermler, H. Michel, Proc. Natl. Acad. Sci. USA 94 (1997) 10547–10553.
- [12] G.T. Babcock, M. Wikström, Nature 356 (1992) 301–309.
- [13] S. Ferguson-Miller, G.T. Babcock, Chem. Rev. 96 (1996) 2889–2907.
- [14] M.I. Verkhovsky, J.E. Morgan, A. Puustinen, M. Wikström, Biochemistry 35 (1996) 16241–16246.
- [15] M. Oliveberg, P. Brzezinski, B.G. Malmström, Biochim. Biophys. Acta 977 (1989) 322–328.

- [16] P. Ädelroth, M. Ek, P. Brzezinski, *Biochim. Biophys. Acta* 1367 (1998) 107–117.
- [17] A. Puustinen, M.I. Verkhovsky, J.E. Morgan, N.P. Belevich, M. Wikström, *Proc. Natl. Acad. Sci. USA* 93 (1996) 1545–1548.
- [18] M. Svensson Ek, P. Brzezinski, *Biochemistry* 36 (1997) 5425–5431.
- [19] B.C. Hill, *J. Biol. Chem.* 266 (1991) 2219–2226.
- [20] M. Svensson-Ek, J.W. Thomas, R.B. Gennis, T. Nilsson, P. Brzezinski, *Biochemistry* 35 (1996) 13673–13680.
- [21] P. Ädelroth, M. Svensson Ek, D.M. Mitchell, R.B. Gennis, P. Brzezinski, *Biochemistry* 36 (1997) 13824–13829.
- [22] I.A. Smirnova, P. Ädelroth, R.B. Gennis, P. Brzezinski, *Biochemistry* 38 (1999) 6826–6833.
- [23] B.L. Trumpower, R.B. Gennis, *Annu. Rev. Biochem.* 63 (1994) 675–716.
- [24] J.E. Morgan, M.I. Verkhovsky, A. Puustinen, M. Wikström, *Biochemistry* 34 (1995) 15633–15637.
- [25] P. Brzezinski, P. Ädelroth, *J. Bioenerg. Biomembr.* 30 (1998) 99–107.
- [26] M. Teixeira, R. Batista, A.P. Campos, C. Gomes, J. Mendes, I. Pacheco, S. Anemuller, W.R. Hagen, *Eur. J. Biochem.* 227 (1995) 322–327.
- [27] G.L. Liao, G. Palmer, *Biochim. Biophys. Acta* 1274 (1996) 109–111.
- [28] A. Aagaard, G. Gilderson, C.M. Gomes, M. Teixeira, P. Brzezinski, *Biochemistry* 38 (1999) 10032–10041.
- [29] W.H. Vanneste, *Biochemistry* 5 (1966) 838–848.
- [30] M.I. Verkhovsky, J.E. Morgan, M. Wikström, *Biochemistry* 33 (1994) 3079–3086.
- [31] J.A. Bailey, C.A. James, W.H. Woodruff, *Biochem. Biophys. Res. Commun.* 220 (1996) 1055–1060.
- [32] Ó. Einarsdóttir, R.B. Dyer, D.D. Lemon, P.M. Killough, S.M. Hubig, S.J. Atherton, J.J. Lopez-Garriga, G. Palmer, W.H. Woodruff, *Biochemistry* 32 (1993) 12013–12024.
- [33] D.D. Lemon, M.W. Calhoun, R.B. Gennis, W.H. Woodruff, *Biochemistry* 32 (1993) 11953–11956.
- [34] C. Varotsis, D.H. Kreszowski, G.T. Babcock, *Biospectroscopy* 2 (1996) 331–338.
- [35] S. Hirota, T. Mogi, T. Ogura, T. Hirano, Y. Anraku, T. Kitagawa, *FEBS Lett.* 352 (1994) 67–70.
- [36] D.A. Proshlyakov, M.A. Pressler, G.T. Babcock, *Proc. Natl. Acad. Sci. USA* 95 (1998) 8020–8025.
- [37] M. Karpefors, P. Ädelroth, A. Aagaard, I.A. Smirnova, P. Brzezinski, *Isr. J. Chem.* 39 (1999) 427–437.
- [38] T. Soulimane, G. Buse, G.P. Bourenkov, H.D. Bartunik, R. Huber, M.E. Than, *EMBO J.* 19 (2000) 1766–1776.
- [39] M.W. Mather, P. Springer, S. Hensel, G. Buse, J.A. Fee, *J. Biol. Chem.* 268 (1993) 5395–5408.
- [40] K. Hon-Nami, T. Oshima, *Biochemistry* 23 (1984) 454–460.
- [41] M.M. Pereira, M. Santana, C.M. Soares, J. Mendes, J.N. Carita, A.S. Fernandes, M. Saraste, M.A. Carrondo, M. Teixeira, *Biochim. Biophys. Acta* 1413 (1999) 1–13.
- [42] A. Kannt, T. Soulimane, G. Buse, A. Becker, E. Bamberg, H. Michel, *FEBS Lett.* 434 (1998) 17–22.
- [43] K. Nikaido, J. Sakamoto, S. Noguchi, N. Sone, *Biochim. Biophys. Acta* 1456 (2000) 35–44.